NASA Technical Paper 2062

November 1982

Film-Cooling Effectiven With Developing Coolan Flow Through Straight a Curved Tubular Passages

S. Stephen Papell,
Chi R. Wang, and
Robert W. Graham

NASA

NASA
Technical
Paper
2062

1982

Film-Cooling Effectiveness With Developing Coolant Flow Through Straight and Curved Tubular Passages

S. Stephen Papell,
Chi R. Wang, and
Robert W. Graham
Lewis Research Center
Cleveland, Ohio

National Aeronautics
and Space Administration

**Scientific and Technical
Information Branch**

Summary

The data were obtained with an apparatus designed to determine the influence of tubular coolant passage curvature on film-cooling performance while simulating the developing flow entrance conditions more representative of cooled turbine blading. Data comparisons were made between straight and curved single tubular passages embedded in the wall and discharging at a 30° angle in line with the tunnel flow. The results showed an influence of curvature on film-cooling effectiveness that was inversely proportional to the blowing rate.

At the lowest blowing rate of 0.18, curvature increased the effectiveness of film cooling by 35 percent; but at a blowing rate of 0.76, the improvement was only 10 percent. In addition, the increase in the film-cooling area coverage ranged from 100 percent down to 25 percent over the same blowing rates.

A data trend reversal at a blowing rate of 1.5 showed the straight tubular passage's film-cooling effectiveness to be 20 percent greater than that of the curved passage with about 80 percent more area coverage.

An analysis of turbulence intensity data in the mixing layer in terms of the position of the mixing interface relative to the wall supported the concept that passage curvature tends to reduce the diffusion of the coolant jet into the main stream at blowing rates below about 1.0. Explanations for the film-cooling performance of both test sections were made in terms of differences in turbulence structure and in secondary flow patterns within the coolant jets as influenced by flow passage geometry.

Introduction

Film cooling is being used in the most advanced turbine designs to maintain tolerable wall temperatures of both stator vanes and rotor blades. The effectiveness of this cooling method is greatly determined by the rate of mixing of the coolant gas with the hot combustion gases that drive the turbine. Rapid dispersal of the coolant gas into the hot stream eliminates its protective capability. Consequently, one method of improving the effectiveness of film cooling is to reduce the mixing so that the coolant stream retains its protective capability for greater distances. One way for effecting such control is reported in reference 1, in which it is shown that curvature of the coolant tube improves film-cooling effectiveness for a range of flow conditions. This improvement is suggested to be the result of modification of the turbulent structure within the coolant stream by the curved tube. Research experience with curved tubes or channels has shown that convex curvature reduces the local turbulence along the convex wall. In the film-cooling application the coolant follows a convex surface before it is ejected into the free-stream hot gases. It is suggested in reference 1 that the convex curvature modifies the turbulence of that portion of the coolant stream that is in contact with the wall and thus enables the stream to adhere longer. It is also suggested that the secondary flows developed in the curved tube contribute to improvements in the coolant effectiveness.

The curved-tube test section reported in reference 1 comprised an adiabatic plate with the curved tube mounted externally to the film-cooling hole. The film-cooling hole was drilled through the plate at a 30° angle to the surface and in line with the tunnel flow. For both the curved and straight tubes compared in reference 1, the coolant tube entrance length to diameter ratio ℓ/d was great enough to produce fully developed flow. Because a coolant passage geometry such as this is not realistic for turbine blading, two new test sections were built with coolant passages embedded within the test plates. The straight and curved passages were then each supplied with coolant from a plenum in contact with the bottom of the test plate to provide a short coolant flow development entrance length more representative of turbine blading coolant passage geometry.

The present experiment differed from that reported in reference 1 in several ways. The tunnel used in this study was the same, but the adiabatic natures of the test plates used in the investigations were quite different. In reference 1 the insulated back side of the plate was exposed to ambient temperatures; in this study the back side of the plate was exposed to the coolant temperature within the plenum. In addition, turbulence intensity data were also obtained in this study to characterize the mixing layer produced by the coolant jet and the tunnel flow.

The purpose of this study therefore was to determine the influence of tubular coolant passage curvature on film-cooling performance while simulating the flow development entrance conditions more representative of cooled turbine blading design geometry. Reported herein are the thermal film-cooling footprints observed by infrared imagery for straight and curved coolant passages embedded in adiabatic test plates. The blowing rates varied from 0.18 to 1.51 and the average temperature difference between the coolant and the tunnel airflow was 22 deg C. Selected hot-wire and total pressure surveys of the flow at the coolant tube discharge and downstream of it are also reported.

Symbols

d	coolant tube diameter
E	dc voltage
e	ac voltage rms

ℓ	coolant tube length
M	blowing rate, $(\rho U)_c/(\rho U)_\infty$
Re	Reynolds number, $\rho Ud/\mu$
T	temperature
Tu	turbulence intensity, $\sqrt{(u')^2/U}$
t	adiabatic plate thickness
U	mean velocity
u'	fluctuating velocity
x	distance from downstream edge of coolant injection port
x/d	dimensionless distance
y	height above test plate
y/d	dimensionless height
η	adiabatic film-cooling effectiveness, $(T_\infty - T_{aw})/(T_\infty - T_c)$
μ	viscosity
ρ	density

Subscripts:

aw	adiabatic wall
b_0	bridge output at zero velocity
c	coolant
∞	free stream or tunnel air
b	bridge output

Apparatus

Figure 1 is a schematic drawing of the test setup. The principal components included the tunnel, the test section–plenum assembly, a Hilsch tube for coolant air supply, and an infrared camera.

The tunnel itself, designed for flow visualization, was made of clear plastic sections with a flow area cross section of 15 by 38 cm. One of the tunnel sections was designed to accept the test plate containing the coolant injection passage as part of the floor of the tunnel. A contoured inlet and a transition piece connected to the altitude exhaust system of the laboratory completed the tunnel assembly.

The tunnel section containing the test plate was positioned so that the developing tunnel boundary layer had about 1.3 m of tunnel length (not including the contoured inlet) in front of the coolant injection port. A replaceable part of the top wall of the tunnel section was designed to accept probes that could be indexed both axially and laterally over the test plate. Velocity profiles obtained by both hot-wire and pitot-tube probes assured the establishment of fully developed turbulent flow. Under the flow conditions of this study, the tunnel flow boundary layer thickness was about 1.65 cm and the turbulence intensity of the free stream was about 3 percent.

The straight and curved coolant passage geometries used in this study are shown schematically in figure 2. Both passages had flow diameters of 1.27 cm and discharged the coolant at an angle of 30° with respect to the surface, which was in line with the tunnel flow. The curved passage was formed by using the lost-wax process in a cast epoxy plug that was embedded in the wall of the test section. A 2.54-cm radius of curvature of the curved coolant channel (fig. 2), which turned the flow through about 95°, was considered to be an optimum geometry (ref. 1) to influence the coolant flow.

The test plates were made of mahogany with a thickness of 6.35 cm to minimize heat transfer through them. In addition, the thick plate also provided a ratio of thickness to coolant passage diameter t/d of 5, which is typical of cooled turbine blade geometry. The surfaces of both plates were finished smooth and painted a dull black. Attached to the test plate was the plenum, through which the coolant air was supplied to the coolant passage at very low velocity. The plenum assembly contained a system of baffles and screens and was covered with fiberglass insulation.

A very adaptable and convenient method for supplying cooling air to the plenum at an appreciable temperature difference below room temperature was the employment of a Hilsch tube. This device, which incorporates a vortex generator element, separates the inlet air into hot and cold streams. This comes about from the forced-vortex or wheel type of angular velocity imparted to the air introduced into the device. Conservation of total energy of the inner portion of the forced vortex causes heat to be transferred to the outer region. Consequently, a relatively cold inner core of air and a warm outer ring of air are available. In the Hilsch tube design the warm- and cold-air discharge ports are on opposite sides of the device. Cold-side temperatures of 0° C could be readily obtained with this device so that temperature differences between the tunnel and coolant air of about 22 deg C could be attained.

The tunnel air temperature was measured with a thermocouple mounted in the contoured inlet. The coolant air temperature was measured with a thermocouple mounted in the inlet plenum between the screens and the mahogany test plate. The coolant airflow rate was measured with a turbine type of flowmeter installed between the Hilsch tube and the coolant plenum. Checks were made to assure that no external leaks occurred in the coolant supply and plenum system.

Turbulence intensity measurements were made with a single-sensor tungsten hot-wire probe. The probe was mounted so that the axis of the sensor was parallel to the test plate and perpendicular to the direction of tunnel flow. The probe was connected to a constant-temperature anemometer, and measurements were taken from a position above the plate of 0.004 diameter out into the crossflow. Turbulence intensity profiles were thus obtained with and without blowing for selected test conditions.

Figure 3 shows the test facility and the method used for turning the infrared radiation. A front-silvered mirror was positioned at a 45° angle to reflect the radiation from the surface of the test plate through the top wall of the tunnel to the detector. A plastic thin-film window was used to minimize radiation absorption.

The infrared camera and detector unit used to measure the surface temperature downstream of the coolant injection port was capable of operating within the temperature range −30° to 200° C and could discriminate temperature differences as small as 0.2 deg C. The detector element was indium antinomide cooled by a liquid-nitrogen bath. The detector displayed the isotherm image on the cathode-ray screen, from which it was then photographed for a permanent record. A reference isotherm at a known temperature was obtained for each data run by focusing the camera on the test plate at a position not influenced by the cooling air jet. The temperature at this position was measured with thermocouples embedded in the plate.

Examples of the photographic data are shown in figure 4. The light gray area in the top photograph represents the 17° C reference isotherm covering most of the plate. The dark area in the center of the photograph is the imprint of the colder film-cooling footprint. The bottom photograph shows a 12° C isotherm downstream of the coolant injection port, which lies within the film-cooling footprint. The temperatures of the isotherm traces are indicated in thermal scale units along the abscissa on the photographs. The scale reading on the bottom of the top photograph represents the known reference temperature, and the difference in scale reading between the photographs represents the temperature difference of the isotherm traces. The two vertical lines on the photographs are the field-of-view limits of the infrared detector. For a given test condition, about six isotherms were photographed, and from these a composite picture (fig. 5) of the film-cooling footprint could be made.

Experimental Procedure and Data Reduction

The experimental data obtained for this study enabled the evaluation of film-cooling effectiveness and turbulence intensity profiles downstream of the coolant injection port. The controlled parameters for these tests were tunnel air velocity, coolant velocity, and coolant temperature. The coolant temperature, measured in the plenum, was set near 0° C. The tunnel air temperature, depending on ambient conditions, was about 25° C. Variations in the blowing rate were obtained by control of tunnel and Hilsch tube airflow values.

After a desired blowing rate was established, the tunnel was permitted to run for about 45 min to attain equilibrium conditions before data collection commenced. A series of isotherm traces on film were then obtained with the infrared camera over the temperature range of the film-cooling footprint. The same testing procedure was repeated over a range of blowing rates for both the straight and curved coolant passage configurations.

The film-cooling effectiveness of each isotherm trace was calculated as

$$\eta = \frac{T_\infty - T_{aw}}{T_\infty - T_c} \tag{1}$$

where T_∞, T_c, and T_{aw} are temperatures of the tunnel air, coolant, and wall, respectively. Information gained from these traces included isotherm temperatures and interpretations of isotherm shapes with regard to the mixing processes of both air streams.

Two types of measurements were obtained from the isotherm photographs. The first measurement was the centerline length of each isotherm trace measured from the edge of the coolant injection port. The second measurement, performed with a planimeter, was the surface area enclosed by the isotherm.

Turbulence intensity profiles with and without blowing were computed from the dc and ac voltage output of the hot-wire probe by using the following relation from reference 2:

$$\mathrm{Tu} = \frac{\sqrt{\overline{(u')^2}}}{U} = \frac{4E_b e_b}{E_b^2 - E_{b0}^2} \tag{2}$$

Data were obtained at selected blowing rates from the plate out into the free stream at various positions along the film-cooling footprint.

Results

Centerline Effectiveness Comparisons

Distributions of film-cooling effectiveness downstream of the coolant injection port are presented in figure 6 for both straight and curved coolant passages. The range of data includes free-stream velocities from 15.3 to 45.9 m/s and coolant velocities from 7.6 to 21.6 m/s. The blowing rate ranged from 0.18 to 1.51. The data are plotted in figure 6 as film-cooling effectiveness in terms of dimensionless distance along the centerline from the edge of the coolant injection port.

Data trends were obtained from differences in slopes and effectiveness levels of the curves relative to each other. An examination of figure 6 shows that at blowing rates below 0.38 the effectiveness level maximized at the coolant injection port and decreased monotonically with distance from the port. At higher blowing rates the curves maximized about 2 to 4 diameters downstream from the port. This position shift in effectiveness maximization was caused by a boundary layer separation bubble forming just downstream of the coolant injection port. It is suggested that the maximization occurred where the boundary layer reattached to the plate.

The film-cooling effectiveness data trends for the straight and curved coolant passages as presented in figure 6 are a function of blowing rate. At the lower blowing rates of 0.18, 0.28, and 0.38, the superior performance of the curved passage over the straight passage is evident. As the blowing rate was increased to about 0.5, figures 6(c), (e), and (g) show the flow separation previously described, as evidenced by the positive slope of the curves near the coolant injection port. In addition, the straight coolant passage was then more effective than the curved passage up to the peaks in the curves. Further downstream the slope of the curve became negative, and once again the curved-passage performance was better than that of the straight passage.

At a blowing rate of 0.76, figure 6(f) shows that the peak values of the curves extended further downstream because of the increased flow separation. In addition, it is suggested that the further decrease in peak values of both curves was caused by coolant penetrating the boundary layer into the free stream and not returning to the plate. Both curves coincide up to about 4 diameters from the coolant injection port, but further downstream the curved passage was once again more effective than the straight passage.

At a blowing rate of 1.09 (fig. 6(h)) the data trend continued with a further decrease in effectiveness over the entire length of the film-cooling footprint. The similarity of the data curves on the plot show that the film-cooling performances of both the straight and curved coolant passages were the same under these flow conditions.

The final set of curves, figure 6(i) at a blowing rate of 1.51, show the continuation of the decrease in effectiveness with increased blowing rate. But, in addition, a reversal in the relative position of the data occurs, with the performance of the straight passage being better than that of the curved passage over the entire length of the film-cooling footprint.

The basic data are crossplotted in figures 7(a) and (b), which represent the straight- and curved-passage data, respectively. The effectiveness is plotted against the blowing rate, and the lines connecting the data are for constant values of x/d from 1 to 13. These curves show the maximization of effectiveness occurring between blowing rates of 0.4 and 0.5. This maximization agrees with published data, as reported, for example, in reference 3. The data in figure 7 cover a range of tunnel velocities from 15.3 to 45.9 m/s; and although tunnel velocity was not used as a plotting parameter, it should be noted that this range of velocities definitely influenced the data. The basic data shown in figure 6 and also reported in reference 4 show a trend in the level of the data curves that increased with increasing tunnel velocity when comparisons were made the traditional way on the basis of blowing rates. Consequently, the shape and level of the curves in figure 7 are unique for only this particular set of data.

For this study the differences between the sets of data are significant, and the magnitude of these differences is summarized in figure 8. The percent difference in film-cooling effectiveness between the straight- and curved-passage data is plotted in figure 8 against the blowing rate as a function of dimensionless distance downstream of the coolant injection port from x/d of 1 to 13. The data curves are for specific values of x/d. For positive values of percent difference the curved passage gave better film-cooling performance than the straight passage, while at negative values the straight passage was better.

An examination of figure 8 shows an increase in effectiveness due to curvature at the lower blowing rates of 0.18, 0.28, and 0.38 that ranged from about 35 percent down to about 10 percent. At a blowing rate of about 0.5 a change in the data is observed. Near the coolant injection port the straight passage was about 5 percent more effective, while farther downstream the curved passage was about 7 percent more effective. An increase in blowing rate to 0.76 shows an average 10 percent increase in effectiveness due to curvature; this increase decreased to zero at a blowing rate of 1.10. With the blowing rate increased to 1.51 the data trend reversed over the entire length of the film-cooling footprint, with the straight passage being about 20 percent more effective than the curved passage. This phenomenon of data reversal at blowing rates of 0.5 and 1.51 has previously been reported with the test geometry used in reference 1.

Film Cooling Coverage Comparison

In the previous section of this report the film-cooling performances of the straight- and curved-passage geometries were examined in terms of the centerline length of the isotherm traces. In this section the data comparisons are extended to the area enclosed by the isotherm trace, defined as its film-cooling coverage.

Differences in film-cooling coverage with the two coolant inlet geometries under the same test conditions are shown in figure 9. The area of the surface enclosed by an isotherm is plotted as a function of film-cooling effectiveness for that particular isotherm. An examination of figure 9 shows data trends that are influenced by blowing rates, somewhat similar to the centerline film-cooling data trends.

The improved performance of the curved passage is shown in figures 9(a) to (g) for blowing rates from 0.18 to 0.76. For this range of blowing rates more surface area was cooled with the curved-passage flow than with the straight-passage flow, and the difference was most pronounced at the lowest blowing rate. At a blowing rate of 1.09 (fig. 9(h)) the data curves coincide, while at a blowing rate of 1.51 (fig. 9(i)) a reversal in the data trend occurs, with the performance of the straight passage being better than that of the curved passage.

The magnitude of these differences obtained from figure 9 were averaged over film-cooling values between 0.2 and 0.5 for each data run, and the percent difference in film-cooling coverage as a function of blowing rate was plotted in figure 10. For positive values of percent difference the curved coolant passage performed better than the straight passage, while for negative values the straight passage performed better. An examination of figure 10 shows that the increase in film-cooling coverage due to curvature ranged from about 100 percent at a blowing rate of 0.18 down to zero at a blowing rate of about 1.0. At higher blowing rates data trend reversal occurred so that at a blowing rate of 1.5 the performance of the straight passage was about 80 percent better than that of the curved passage. The dashed line in figure 10 is meant to be only an indication of a trend in the data and not a correlation line.

Tunnel Velocity and Turbulence Intensity (No Blowing)

To characterize the tunnel flow, velocity and turbulence intensity profiles were obtained at a free-stream Reynolds number Re_∞ of 4.3×10^5 for a position just upstream of the coolant injection port with no flow through the coolant passage. The results are presented in figure 11.

A hot-wire probe was used to obtain both velocity and turbulence intensity measurements, and a pitot tube was used for an additional velocity measurement. Both methods produced similar velocity profiles consistent with that of fully developed turbulent flow. The turbulence intensity ranged from about 3 percent at the edge of the boundary layer to 9 percent near the wall.

Centerline Turbulence Intensity (With Blowing)

Turbulence intensity hot-wire data for straight- and curved-passage coolant injection are presented in figures 12 and 13, respectively, for a blowing rate of 0.22. Nine centerline profiles normal to the wall are shown on these figures from a position in front of the coolant injection port at x/d of 1.5 to 7 diameters downstream. The mixing layer lies in the region between the wall at $y/d=0$ and the distance normal to the wall where the turbulence profile differs from the no-blowing case as, for example, shown in figure 12(c). The solid curve on this figure represents the no-blowing turbulence profile obtained from figure 11 for a position just upstream of the coolant injection port ($x/d= -2$). Within the mixing layer each profile maximized at some position y/d above the test plate, as illustrated by the dashed lines in figures 12 and 13.

A measurement of the height y/d of maximum turbulence intensity at each axial location x/d was obtained from figures 12 and 13 for both the straight- and curved-passage data. The data, summarized in figure 14, show that this turbulence maximum was a function of distance from the coolant injection port and increased in value in the downstream direction, indicative of the spreading jet. In addition, it is significant that the inflection in the turbulence profile was closer to the wall for the curved passage than for the straight passage.

Turbulence Intensity at Coolant Injection Port

A survey of turbulence intensity was also made at the the coolant injection port for both straight and curved inlets. Two sets of data are presented in figures 15(a) and (b) for blowing rates of 0.22 and 0.37, respectively. The turbulence intensity was mapped along the centerline of the hole and also along a position midway between the centerline and the edge of the hole.

An examination of figure 15 shows a decreasing trend in the turbulence data along the centerline in the direction of the tunnel flow that is similar for all four data runs. Along the off-centerline profile, though, the influence of channel curvature on the distribution of turbulence is readily apparent in both sets of data. The straight-inlet off-centerline data show a small decrease in turbulence from the centerline values, while the curved-inlet off-centerline data show a relatively large increase in turbulence from the centerline values. This increase in turbulence along the off-centerline profile was probably due to secondary flows caused by channel curvature generating vortices within the coolant passage itself.

Discussion

The improved film-cooling performance of the curved tubular coolant passage over the straight passage has been demonstrated herein for a range of blowing rates relevant to turbine cooling from 0.18 to 0.80. The evidence is presented in terms of isotherm traces obtained under similar test conditions and by corresponding hot-wire measurements of turbulence intensity in the mixing layer. Comparisons of maximum turbulence profiles along the centerline of the test surface revealed that for a blowing rate of 0.22 the mixing layer developed by using the curved-passage geometry was closer to the test surface than the straight-passage mixing layer. It is suggested that maximum turbulence in the boundary layer exists at the interface between the jet and the crossflow. The height of this interface reflects the amount the jet turns toward the wall so that the closer the interface is to the wall the more effective would be the jet in protecting its surface. It is also postulated that the film-cooling performances of both test sections are affected by differences in the turbulence structure and in secondary flow patterns within the jets themselves as influenced by the coolant passage geometry.

Classically, when a wall jet is acted on by a crossflow, the main stream decelerates at the upstream point of contact, resulting in a pressure rise. On the downstream side of the jet a rarefaction occurs, resulting in a pressure drop. The pressure drop across the jet is the force that turns it toward the wall. The energy required to turn the jet comes out of the main-stream flow and is constant for a given flow condition.

The coolant ejected from a straight tubular passage expands, but the streamlines are initially parallel to the injection angle. When acted on by the main stream, vortices are formed (refs. 5 and 6) that spread the jet laterally into the kidney-bean-shape cross section shown schematically in figure 16. The energy for the generation of vortices and the jet turning comes out of the main stream and results in a film-cooling performance that depends on the proximity of the coolant to the wall and the rate of mixing with the main stream.

When a curved tubular passage is used, the secondary flows caused by curvature initiate vortices within the tube itself. The energy to generate these vortices comes from centripetal body forces produced by the passage geometry so that, when this flow is discharged into the main stream, these vortices are already present and do not require initiation by the main stream. Consequently, the main stream has more momentum available to turn the coolant to the wall, resulting in enhanced film-cooling effectiveness specifically for flow conditions at blowing rates below about 1.0.

At blowing rates above about 1.0 the data reversal trend reported herein showed the straight tubular passage to be more effective than the curved passage. Under these flow conditions the momentum of the main stream is relatively low compared with that of the coolant jet so that there is less energy available to turn the jet. Consequently, it is suggested that the rate of mixing between the two streams becomes the predominant mechanism in the destruction of the jet and establishes the level of film-cooling effectiveness available.

Hot-wire measurements at the coolant injection port for blowing rates of 0.22 and 0.37 showed evidence of increased turbulence in the curved passage. Since this type of data was not obtained at the higher blowing rates, it can only be inferred that turbulence, induced by coolant passage curvature for blowing rates above about 1.0, promotes mixing and lowers the film-cooling effectiveness of the jet.

It is important to note that the trends in the present data are similiar to the reference 1 data even though there were some significant test differences. Both sets of data show the improved film-cooling performance of the curved coolant channel over the straight channel at lower blowing rates. At higher blowing rates the data reversal trends described in reference 1 again appear herein, showing the better performance of the straight channel over the curved channel.

Summary of Results

The film-cooling data reported herein were obtained with an apparatus designed to determine the influence of coolant passage curvature on film-cooling performance and to simulate the coolant flow entrance conditions found in cooled turbine blading. Two test plates were used, with the coolant passages embedded in the walls and discharging at an angle of 30° to the surface, which was in line with the free-stream flow. One of the test plates had a straight coolant passage; the other had a curved coolant passage. The coolant entered the flow passage from a plenum in contact with the plates.

The test conditions included blowing rates from 0.18 to 1.51 with average temperature differences of 22 deg C between the tunnel and coolant air. Data comparisons are presented graphically in terms of the centerline length of the isotherms measured from the edge of the coolant injection port, the surface area enclosed by the isotherm film-cooling footprint, and the turbulence intensity profile within the mixing layer.

The following results were obtained while operating both test sections under comparable test conditions.

Centerline Film-Cooling Effectiveness

Over the range of blowing rates M from 0.18 to 0.76, which is of practical interest in turbine cooling, curved-passage film cooling was generally more effective than straight-passage film cooling. Differences in the results ranged from about 35 percent at $M=0.18$ to about 10 percent at $M=0.76$ when averaged over the centerline length of the film-cooling footprint. At the higher blowing rates a reversal in the data trend occurred. At $M=1.5$ the straight-passage effectiveness was better than the curved-passage effectiveness by about 20 percent.

Film-Cooling Coverage

For the range of blowing rates from 0.18 to 0.76, data comparisons of surface area coverage for equaltemperature isotherms showed the superior performance of the curved passage over the straight passage. The increase in area coverage due to curvature ranged from 100 percent at $M=0.18$ to zero at $M=1.0$. At the higher blowing rates the reversal in the data trend shown by the centerline film-cooling effectiveness data also occurred here. At $M=1.5$ the straight-passage data showed an 80 percent increase in film-cooling coverage over the curved-passage data.

Turbulence Intensity

The tunnel flow turbulence intensity for the no-blowing case ranged from 3 percent in the free stream to 9 percent in the boundary layer. At a blowing rate of 0.22 the maximum turbulence intensity in the mixing layer was 11 percent. The location of maximum turbulence intensity in the mixing layer at $M=0.22$ was shown to be closer to the wall for the curved coolant passage than for the straight coolant passage. These maximums are conjectured to be the locii of the mixing interface between the coolant and the free stream. The closer this mixing interface is to the wall, the more effective the coolant is in protecting the wall.

Lewis Research Center
National Aeronautics and Space Administration
Cleveland, Ohio, June 7, 1982

References

1. Papell, S. S.; Graham, R. W.; and Cageao, R. P.: Influence of Coolant Tube Curvature on Film Cooling Effectiveness as Detected by Infrared Imagery. NASA TP-1546, 1979.
2. Hot Wire and Hot Film Measurements and Applications. Technical Bulletin No. 4, Thermo-Systems, Inc., Saint Paul, Minn., 55113.
3. Goldstein, R. J.; Eckert, E. R. G.; and Ramsey, J. W.: Film Cooling with Injection Through a Circular Hole. (HTL-TR-82, Minnesota Univ.; NAS3-7904.) NASA CR-54604, 1968.
4. Goldstein, R. J.; et al.: Film Cooling Following Injection Through Inclined Circular Tubes. (HTL-TR-91, Minnesota Univ., NAS3-7904.) NASA CR-72612, 1969.
5. Abramovich, G. N.: The Theory of Turbulent Jets. M.I.T. Press, 1963.
6. Keffer, J. F.; and Baines, W. D.: The Round Turbulent Jet in a Cross Wind. J. Fluid Mech., vol. 15, no. 4, pp. 481-496, Apr. 1963.

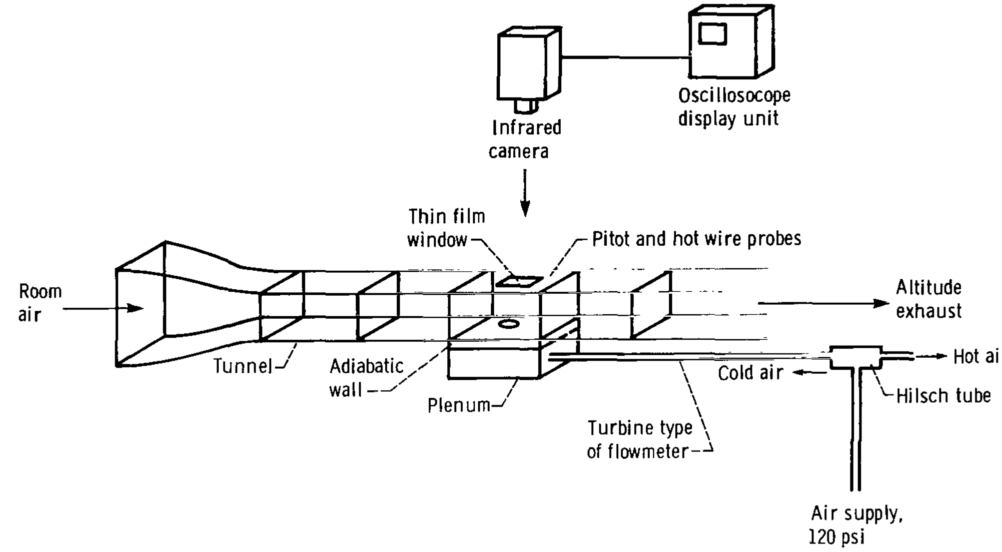

Figure 1. - Schematic drawing of film-cooling rig.

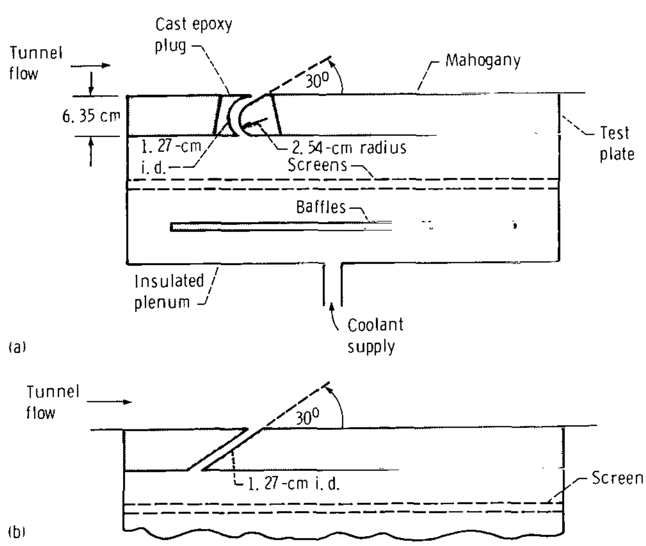

(a) Test plate with curved passage.

(b) Test plate with straight passage.

Figure 2. - Schematic of test plates and coolant supply plenum.

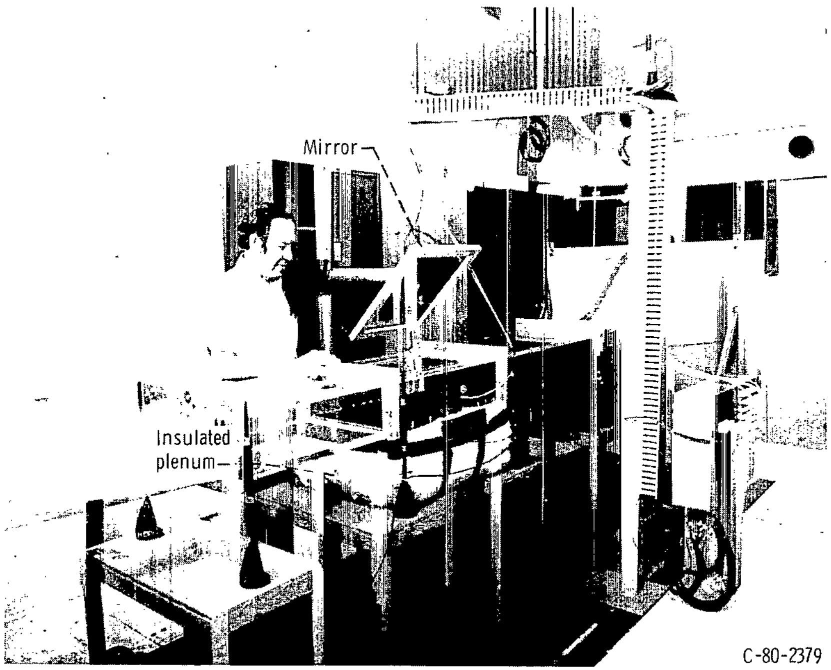

Figure 3. - Tunnel and test section, showing insulated plenum and mirror for turning infrared radiation.

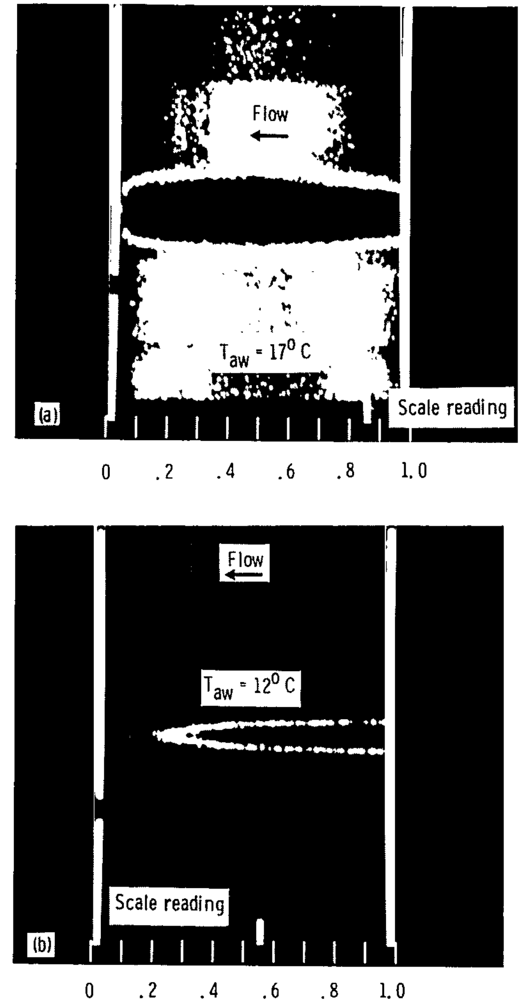

(a) Reference scale reading for measured wall temperature.

(b) Isotherm in film-cooling footprint.

Figure 4. - Isotherm traces.

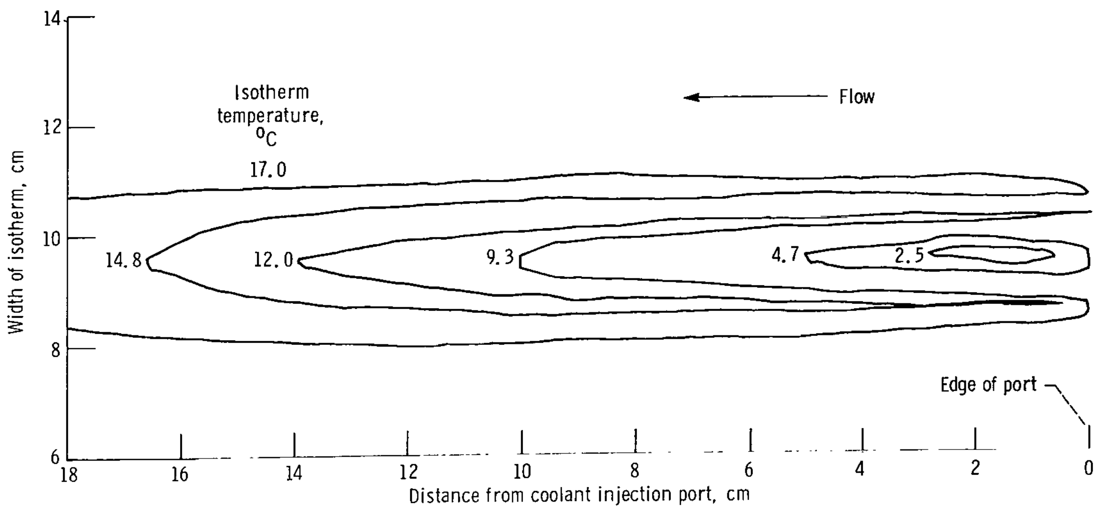

Figure 5. - Film-cooling footprint (isotherm traces) for straight tubular passage injection. Blowing rate, M, 0.38; injection angle, 30°; tunnel air temperature, T_∞ = 19.7° C; coolant temperature, T_c = -3.0° C.

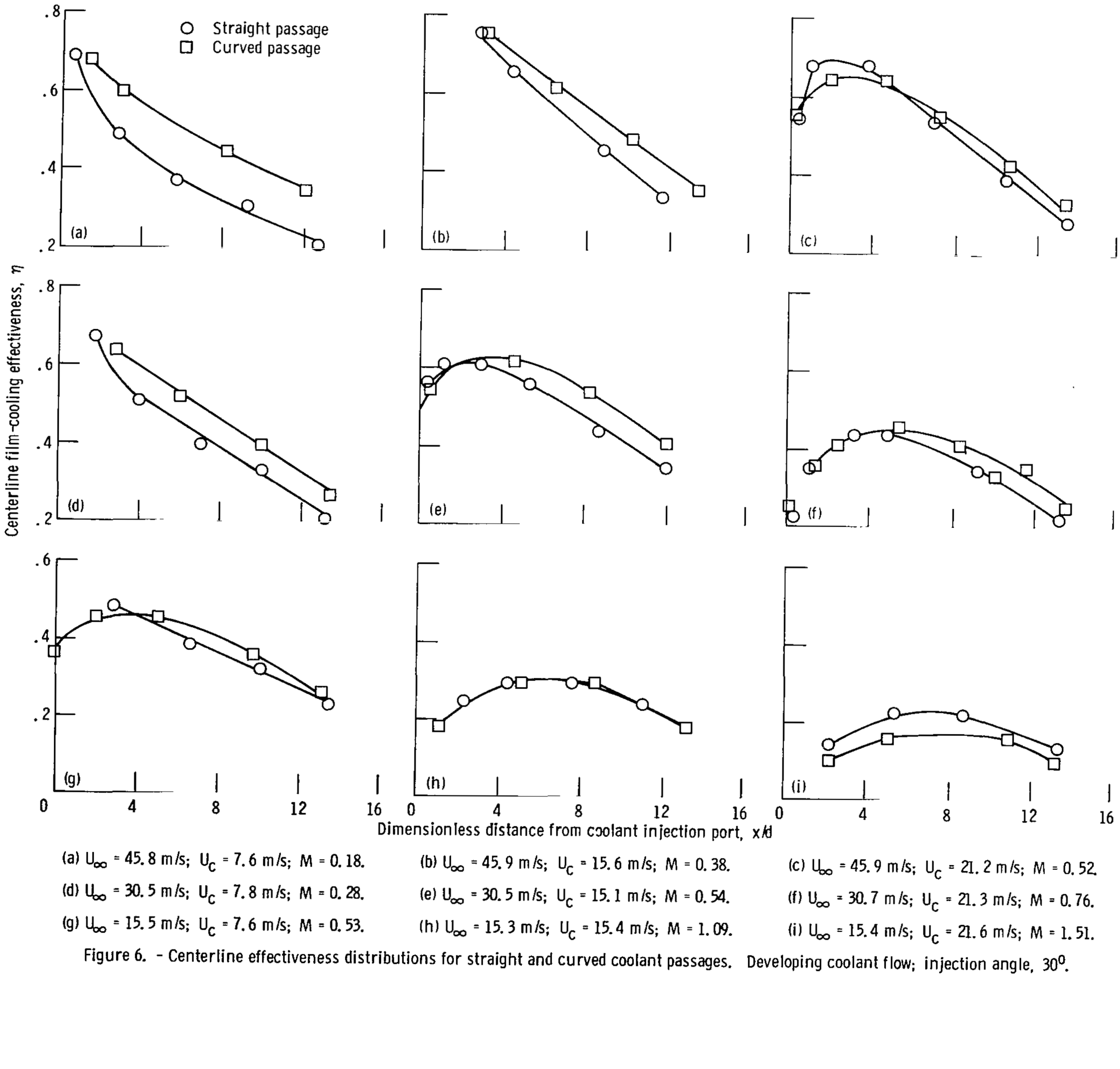

(a) U_∞ = 45.8 m/s; U_c = 7.6 m/s; M = 0.18.
(b) U_∞ = 45.9 m/s; U_c = 15.6 m/s; M = 0.38.
(c) U_∞ = 45.9 m/s; U_c = 21.2 m/s; M = 0.52.
(d) U_∞ = 30.5 m/s; U_c = 7.8 m/s; M = 0.28.
(e) U_∞ = 30.5 m/s; U_c = 15.1 m/s; M = 0.54.
(f) U_∞ = 30.7 m/s; U_c = 21.3 m/s; M = 0.76.
(g) U_∞ = 15.5 m/s; U_c = 7.6 m/s; M = 0.53.
(h) U_∞ = 15.3 m/s; U_c = 15.4 m/s; M = 1.09.
(i) U_∞ = 15.4 m/s; U_c = 21.6 m/s; M = 1.51.

Figure 6. - Centerline effectiveness distributions for straight and curved coolant passages. Developing coolant flow; injection angle, 30°.

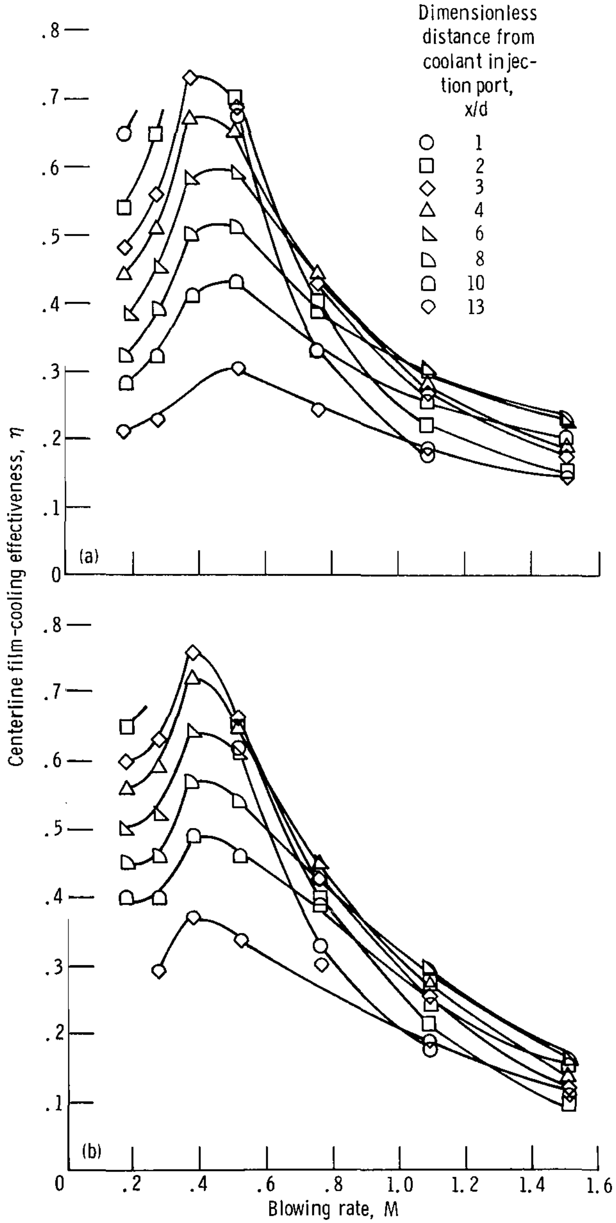

(a) Test plate with straight coolant passage.

(b) Test plate with curved coolant passage.

Figure 7. - Cross plot of figure 6 showing centerline film-cooling data as a function of blowing rate for dimensionless distances from coolant injection port of 1 to 13.

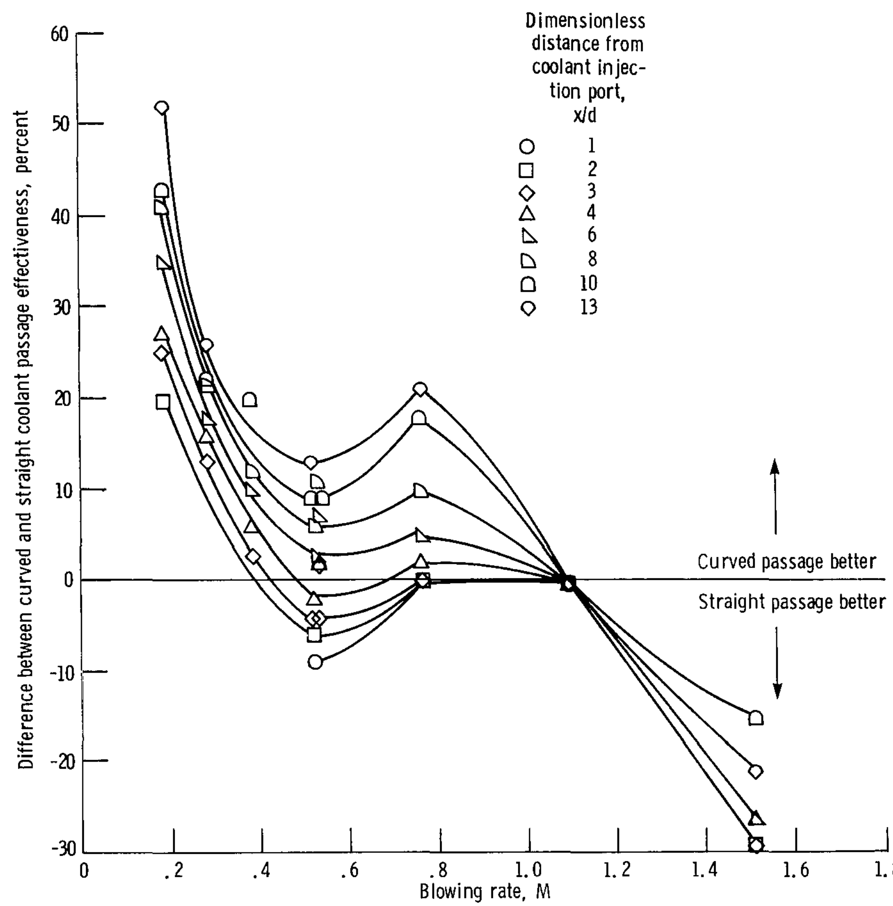

Figure 8. - Influence of coolant inlet geometry on centerline film-cooling effectiveness.

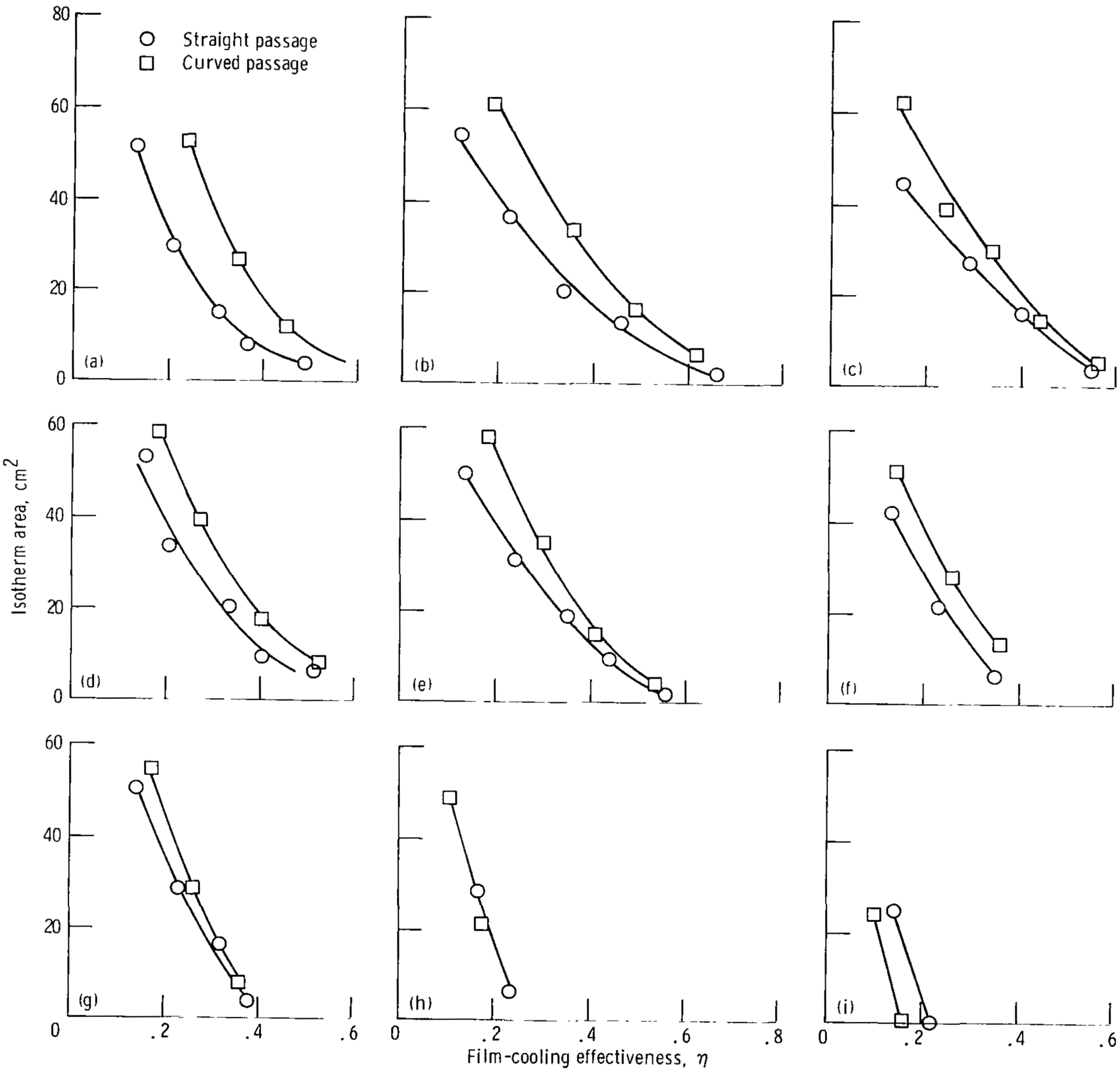

(a) U_∞ = 45.8 m/s; U_c = 7.6 m/s; M = 0.18.

(b) U_∞ = 45.9 m/s; U_c = 15.6 m/s; M = 0.38.

(c) U_∞ = 45.9 m/s; U_c = 21.2 m/s; M = 0.52.

(d) U_∞ = 30.5 m/s; U_c = 7.8 m/s; M = 0.28.

(e) U_∞ = 30.5 m/s; U_c = 15.1 m/s; M = 0.54.

(f) U_∞ = 30.7 m/s; U_c = 21.3 m/s; M = 0.76.

(g) U_∞ = 15.5 m/s; U_c = 7.6 m/s; M = 0.53.

(h) U_∞ = 15.3 m/s; U_c = 15.4 m/s; M = 1.09.

(i) U_∞ = 15.3 m/s; U_c = 21.6 m/s; M = 1.51.

Figure 9. - Isotherm area film-cooling coverage for straight and curved coolant passages. Developing coolant flow; injection angle, 30°.

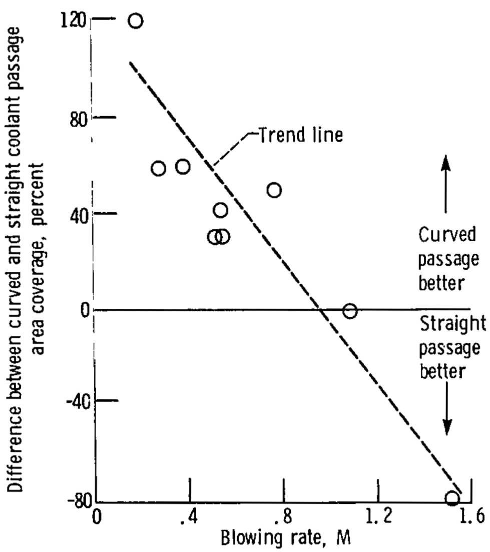

Figure 10. - Influence of coolant inlet geometry on film-cooling coverage.

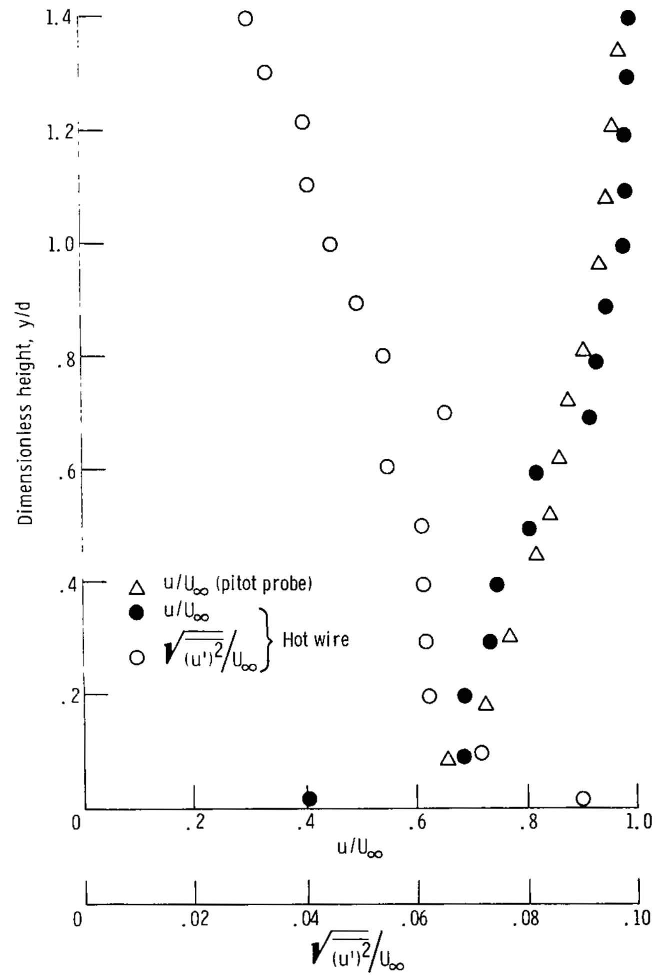

Figure 11. - Tunnel flow turbulence and velocity profiles with no blowing. Mean velocity of tunnel air, U_∞, 23 m/s; Reynolds number, Re, 1.4×10^6/m; dimensionless distance from coolant injection port, x/d, -2.

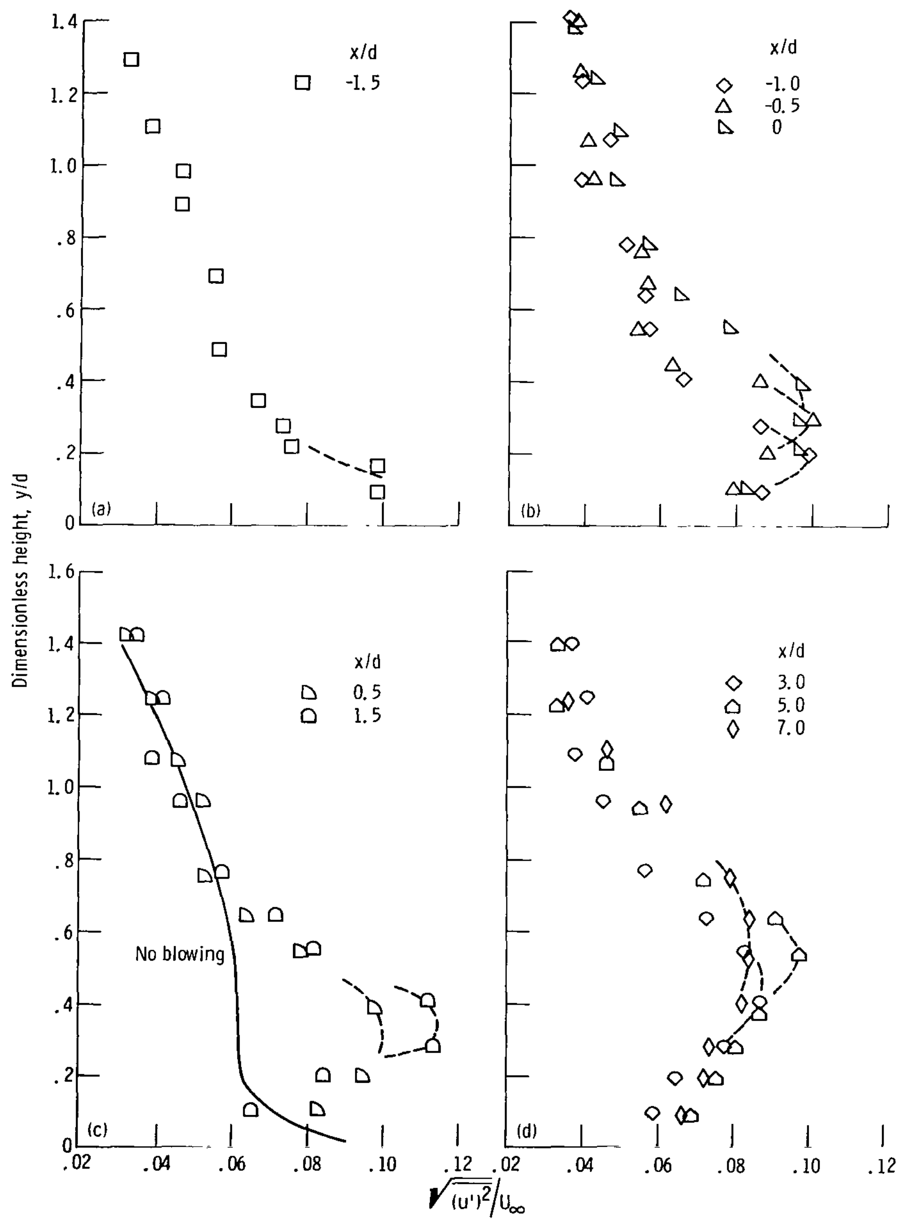

(a) Dimensionless distance from coolant injection port, x/d, -1.5.

(b) Dimensionless distances from coolant injection port, x/d, -1.0, -0.5, and 0.

(c) Dimensionless distances from coolant injection port, x/d, 0.5 and 1.5.

(d) Dimensionless distances from coolant injection port, x/d, 3.0, 5.0, and 7.0.

Figure 12. - Turbulence intensity profiles (centerline) for straight passage at blowing rate M of 0.22

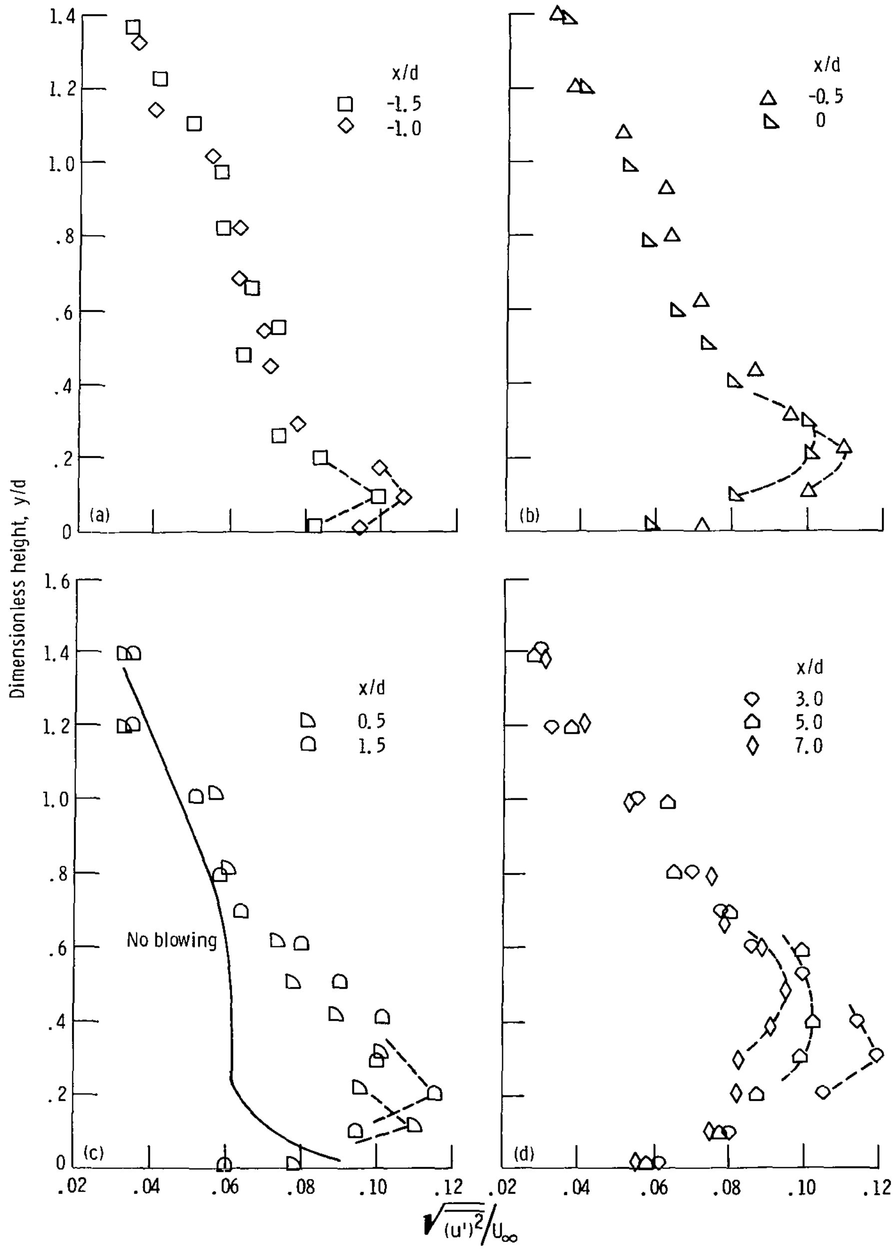

(a) Dimensionless distances from coolant injection port, x/d, 1.5 and 1.0.

(b) Dimensionless distances from coolant injection port, x/d, -0.5 and 0.

(c) Dimensionless distances from coolant injection port, x/d, 0.5 and 1.5.

(d) Dimensionless distances from coolant injection port, x/d, 3.0, 5.0, and 7.0.

Figure 13. - Turbulence intensity profiles (centerline) for curved passage at blowing rate M of 0.22.

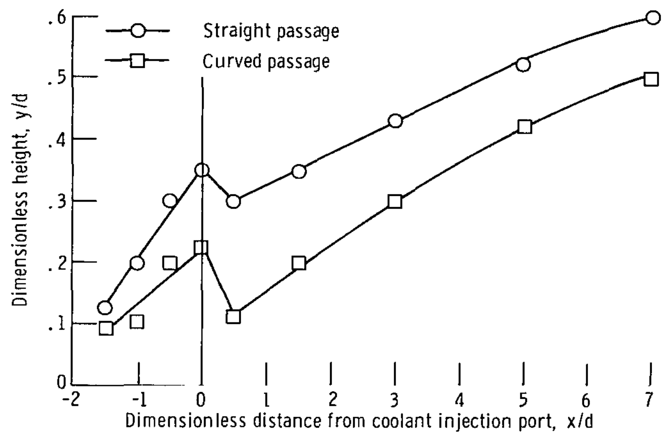

Figure 14. - Centerline dimensionless height above test plate of maximum turbulence intensity in mixing layer for straight and curved coolant injection passages for dimensionless distance from coolant injection port x/d of -1.5 to 7 for blowing rate M of 0.22.

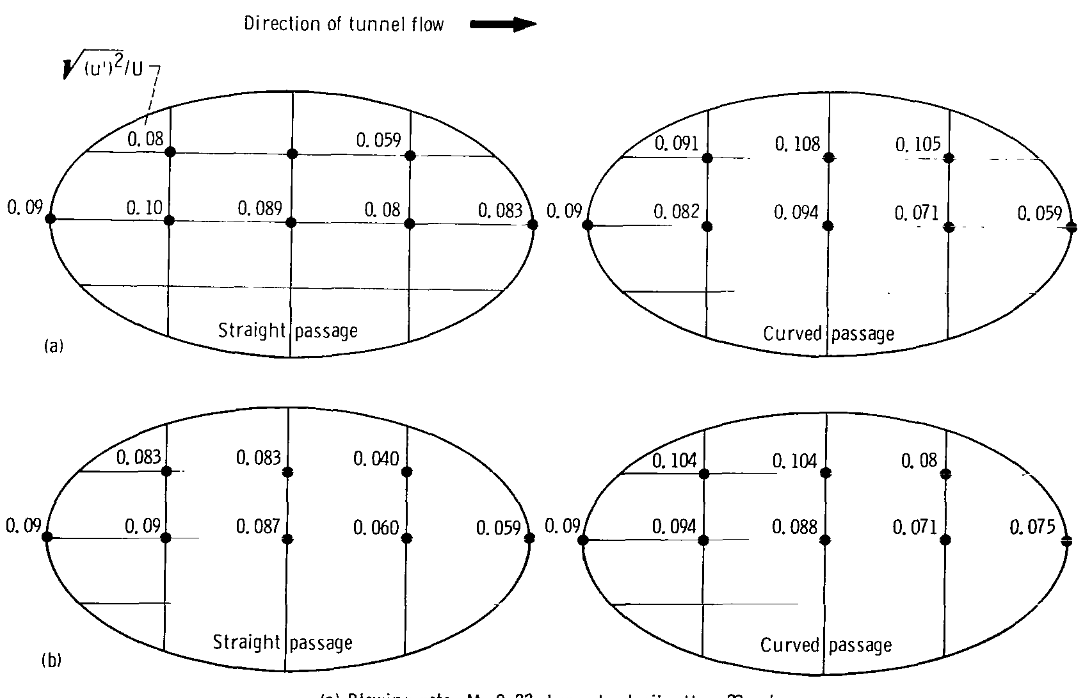

(a) Blowing rate, M, 0.22; tunnel velocity U_∞, 23 m/s.

(b) Blowing rate, M, 0.37; tunnel velocity U_∞, 23 m/s.

Figure 15. - Turbulence intensity at coolant injection port.

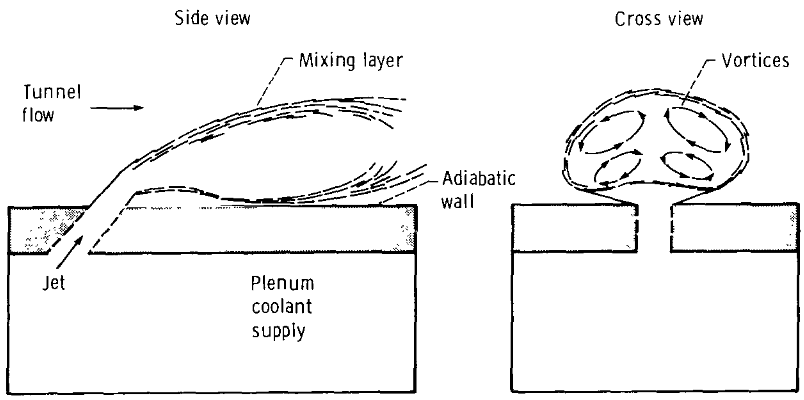

Figure 16. - Schematic drawing of an inclined wall jet subject to crossflow, showing generation of vortex flow.

1. Report No. NASA TP-2062	2. Government Accession No.	3. Recipient's Catalog No.
4. Title and Subtitle FILM-COOLING EFFECTIVENESS WITH DEVELOPING COOLANT FLOW THROUGH STRAIGHT AND CURVED TUBULAR PASSAGES		5. Report Date November 1982
		6. Performing Organization Code 505-32-2B
7. Author(s) S. Stephen Papell, Chi R. Wang, and Robert W. Graham		8. Performing Organization Report No. E-1206
		10. Work Unit No.
9. Performing Organization Name and Address National Aeronautics and Space Administration Lewis Research Center Cleveland, Ohio 44135		11. Contract or Grant No.
		13. Type of Report and Period Covered Technical Paper
12. Sponsoring Agency Name and Address National Aeronautics and Space Administration Washington, D.C. 20546		14. Sponsoring Agency Code

15. Supplementary Notes

16. Abstract

The data were obtained with an apparatus designed to determine the influence of tubular coolant passage curvature on film-cooling performance while simulating the developing flow entrance conditions more representative of cooled turbine blading. Data comparisons were made between straight and curved single tubular passages embedded in the wall and discharging at a 30° angle in line with the tunnel flow. The results showed an influence of curvature on film-cooling effectiveness that was inversely proportional to the blowing rate. At the lowest blowing rate of 0.18, curvature increased the effectiveness of film cooling by 35 percent; but at a blowing rate of 0.76, the improvement was only 10 percent. In addition, the increase in film-cooling area coverage ranged from 100 percent down to 25 percent over the same blowing rates. A data trend reversal at a blowing rate of 1.5 showed the straight tubular passage's film-cooling effectiveness to be 20 percent greater than that of the curved passage with about 80 percent more area coverage. An analysis of turbulence intensity data in the mixing layer in terms of the position of the mixing interface relative to the wall supported the concept that passage curvature tends to reduce the diffusion of the coolant jet into the main stream at blowing rates below about 1.0. Explanations for the film-cooling performance of both test sections were made in terms of differences in turbulence structure and in secondary flow patterns within the coolant jets as influenced by flow passage geometry.

17. Key Words (Suggested by Author(s))	18. Distribution Statement
Film cooling Jet flow Curved passages Turbulence	Unclassified - unlimited STAR Category 34

19. Security Classif. (of this report)	20. Security Classif. (of this page)	21. No. of Pages	22. Price*
Unclassified	Unclassified	22	A02

* For sale by the National Technical Information Service, Springfield, Virginia 22161

NASA-Langley, 1982

National Aeronautics and
Space Administration

Washington, D.C.
20546

Official Business
Penalty for Private Use, $300

THIRD-CLASS BULK RATE

Postage and Fees Paid
National Aeronautics and
Space Administration
NASA-451

U.S.MAIL

5 1 1U,D, 821027 S00903DS
DEPT OF THE AIR FORCE
AF WEAPONS LABORATORY
ATTN: TECHNICAL LIBRARY (SUL)
KIRTLAND AFB NM 87117

NASA

POSTMASTER: If Undeliverable (Section 158
Postal Manual) Do Not Return